

Modelling the Effect of Artificial Mixing on Thermal Stability and Substance Transport in a Drinking-water Reservoir Using a 3D Hydrodynamic Model

Shengyang Chen^{1,3}, Chengwang Lei¹, Cayelan C. Carey², and John C. Little³

¹ School of Civil Engineering, The University of Sydney, Sydney, New South Wales 2006, Australia

² Department of Biological Sciences, Virginia Tech, Blacksburg, Virginia 24061, USA

³ Department of Civil and Environmental Engineering, Virginia Tech, Blacksburg, Virginia 24061, USA

Abstract

A semi-implicit three-dimensional (3D) hydrodynamic model (Si3D) is employed to analyse artificial mixing in a drinking-water reservoir. A recently-developed coupled water-jet model and a previously validated bubble-plume model are used with Si3D to simulate artificial mixing systems in operation. The numerical results are compared against *in-situ* experimental data for model validation purposes. The study aims to identify the effects of mixing induced by the artificial mixing systems on the variation of thermal stability, and to investigate substance transport mechanisms under the influence of artificial mixing over the experimental period. The 3D mixing effects across the reservoir are also visualised and discussed with tracers added into the model.

Introduction

Artificial mixing devices are often deployed to deal with water quality problems in reservoirs, such as algal blooms and hypoxia. Common destratification and oxygenation systems include bubble-plumes, airlift aerators, Speece cones, and side-stream pumping systems. Among the artificial mixing systems, side-stream pumping and bubble plume systems have been shown to successfully mitigate water quality problems by adding oxygen to water bodies.

Both mixing and oxygenation systems change the thermal structure of the water column, which alters the performance of the systems themselves, and can influence substance transport in reservoirs. Studies show that the mixing generally results in an increase of dissolved oxygen in the water, as well as an increase of temperature in the deeper layers of the water bodies, but a decrease in temperature in the upper layers. However, the outcomes of artificial mixing have not always been positive. Mixing induced by a side-stream pumping system, for example, can cause premature destratification of the water column in some cases [7]. Furthermore, Nürnberg et al. [4] showed that improper mixing increased phosphorus transfer from the hypolimnion to the epilimnion, thereby causing surface algal blooms.

To investigate the mixing mechanism involved in system operation, coupled hydrodynamic models are increasingly used. Previous studies using one-dimensional (1D) or two-dimensional (2D) numerical models to investigate artificial mixing may not well resolve the non-homogeneous mixing across water bodies. Adopting three-dimensional (3D) hydrodynamic models can account for the effect of mixing in specific locations and depths of reservoirs, which can achieve higher accuracy for model-predicted results compared to 1D or 2D models.

The present study adopts a semi-implicit 3D hydrodynamic model (Si3D) to analyse artificial mixing induced by a set of water quality management systems comprising a bubble-plume

epilimnetic mixing (EM) system and a side-stream supersaturation (SSS) hypolimnetic oxygenation system. A model for simulating the SSS system (water-jet model) and a bubble-plume model for the epilimnetic mixing system are used to simulate the mixing devices in operation. *In-situ* whole-reservoir experiments are carried out to provide field data for understanding the mixing mechanisms in association with model results. The thermal structure and substance transport across the water body during artificial mixing are the main focus of this study.

Methodology

Study Site

The *in-situ* experiments were carried out in Falling Creek Reservoir (FCR), which is a shallow, eutrophic drinking-water reservoir managed by Western Virginia Water Authority, Virginia, USA (Figure 1). The SSS and EM systems as shown in Figure 1 are deployed in FCR to mitigate hypolimnetic hypoxia and occasional algal blooms during the stratified period with the SSS diffuser at ~ 1-m above the sediment and the EM diffuser at ~ 5-m below the water surface. The diffusers of the SSS and EM systems are installed towards the deeper end of the reservoir as indicated by the white lines in Figure 1.

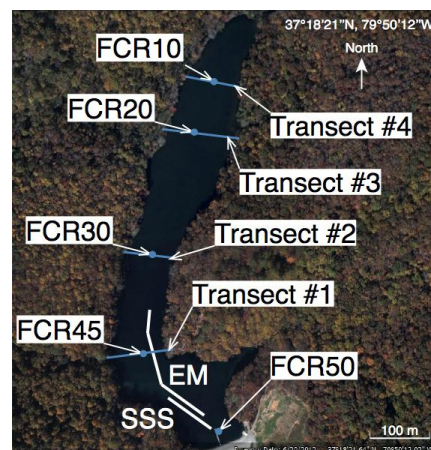


Figure 1 Schematic diagram of sampling locations. The corresponding locations include five single water column profiles (FCR10-50) and four cross-sectional transects across FCR (Transect #1-4).

Field Data Collection

The field experiments were performed during the summer of 2016, with the SSS system in continuous operation during the study period and the EM system operated for 6 hours only (see Table 1). The data collected included water temperature, dissolved oxygen, turbidity, and meteorological data. Field measurements were carried out using an SBE 19plus (Seabird

Electronics, Bellevue, WA, USA) high-resolution (4 Hz sampling rate) Conductivity, Temperature, and Depth (CTD) profiler and a ProODO meter (YSI Inc., Yellow Springs, OH, USA). The CTD was used to collect depth profiles for temperature and dissolved oxygen. The response time of the CTD is 1.4 s at 20°C, facilitating data to be collected in a fine resolution (~0.1-m increments) in the water column. The ProODO meter was used to check the quality of the temperature and oxygen data collected using the CTD, with lower sampling frequency at ~1.0 m from the water surface to 9 m depth. The field data were processed following the procedures described in [1]. The meteorological data required for the numerical modelling were obtained from an *in-situ* weather station (CR3000: Micrologger, Campbell Scientific Inc, UT, USA) deployed at the dam of FCR. The sampling interval of the weather station was one minute. The quality of the data was checked against the meteorological data from Roanoke Airport, 11.8 km away from FCR, which was downloaded from the National Climatic Data Center, National Oceanic and Atmospheric Administration (NOAA, www.ncdc.noaa.gov/).

Day of Year 2016	146-149	150	151	152
SSS	ON @ ~ 200 LPM			
EM		ON		
		@ 25 scfm for 6 hours		

Table 1 Experimental schedules.

Numerical Models

The Si3D hydrodynamic model adopts a finite-difference method for numerical solution of Navier-Stokes equations [5]. The numerical grid for Si3D is generated based on the FCR bathymetry (see Figure 2).

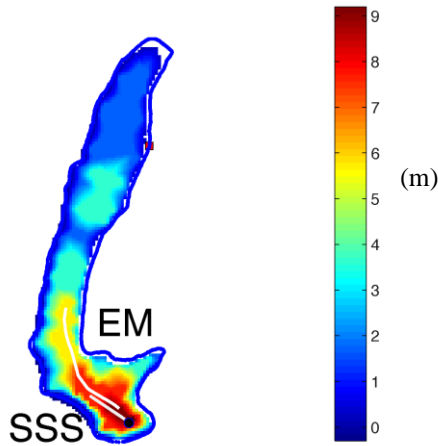


Figure 2 FCR bathymetry in the Si3D hydrodynamic model.

Water-jet and bubble-plume models are the two models coupled in Si3D, which resolve the flows induced by artificial mixing. The two models have been designed to work simultaneously in Si3D, which enables the prediction of the complex mixing induced by the two different systems.

The coupled water-jet model resolves the small-scale jet flow with the much larger grid cells in the hydrodynamic model. The water-jet model was developed based on a jet flow theory [3]. As shown in Figure 3a, the coupled water-jet model accounts for the ambient flow induced by the nozzle and the discharge of the oxygen-rich water from the nozzle. In addition to the momentum

induced by the jet discharge, the model also resolves the ambient flow entrained by the expanding jet.

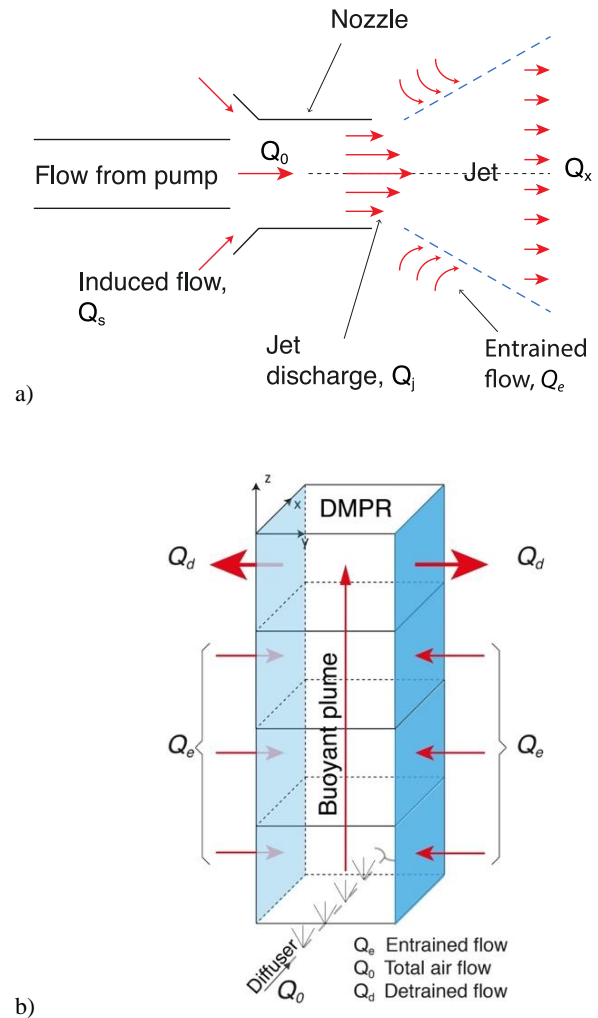


Figure 3 a) Diagram of flows from a water jet; b) Schematic diagram of flows induced by the bubble-plume model.

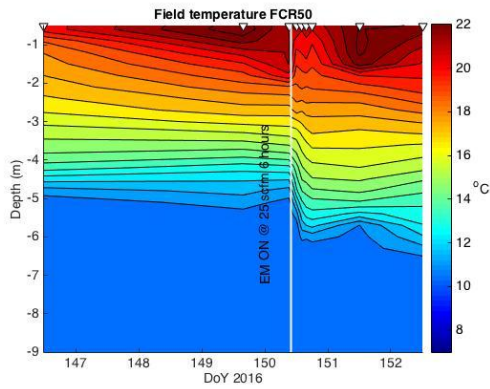
A linear bubble-plume model was employed to simulate the flow of the EM system, which releases air bubbles from a diffuser line within the thermocline. The theory behind the bubble-plume model has been well established (e.g. [6]), with a schematic representation of the model provided in Figure 3b. The model successively relocates the water with entrainment from the lower cell to the upper cell until the depth of maximum plume rise is reached, where the plume water is detrained horizontally into the adjacent grid cells.

Results and Discussion

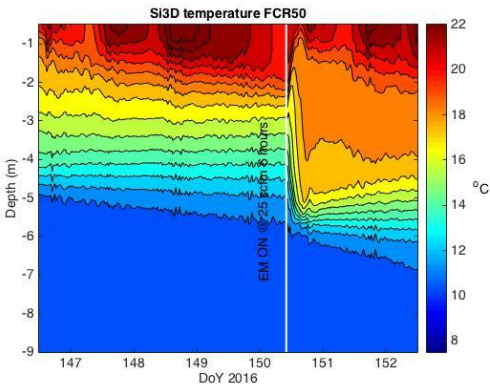
Both experimental and numerical results are described to identify the effects of the artificial mixing on the thermal structure and substance transport across FCR.

Temperature

The time series of the temperature evolution at FCR50 obtained from the experiment and simulation are shown in Figure 4. When focusing on the continuous operation of the SSS system only from Day 146 to Day 149, it can be observed in the temperature contours that the thermal structure of the water column was barely altered, which is consistently predicted by the numerical model. However, the 6-hour operation of the EM system on day 150 deepened the thermocline significantly, which results in a distinct change in the thermal stability of the reservoir.

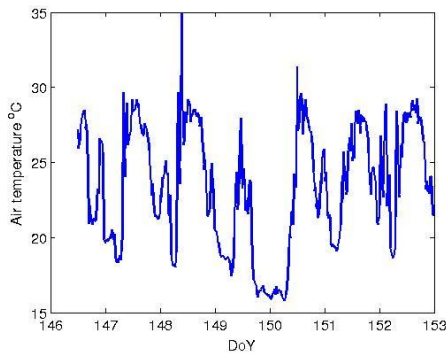


a)

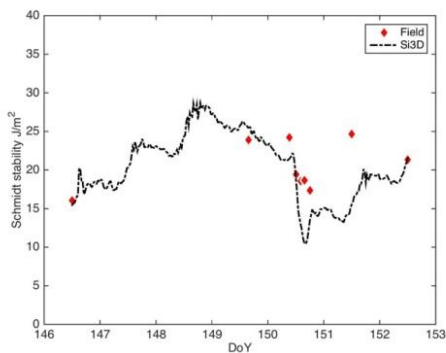


b)

Figure 4 Contours of the time series of temperature evolution at FCR50: a) Experiment; triangles on top indicate the sample dates; b) Simulation.



a)



b)

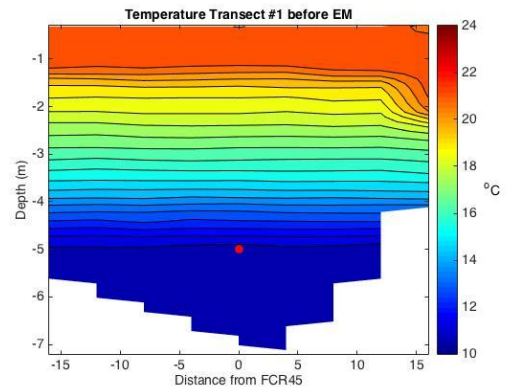
Figure 5 a) Air temperature above water surface during the study period. b) Time series of Schmidt stability obtained from the experiment and simulation.

To analyse the thermal stability of the water body, the concept of Schmidt stability [2] is adopted. The Schmidt stability estimates the potential energy inherent in the stratified water that resists mechanical mixing. The stability in the reservoir (Figure 5b) is calculated for both the experimental and numerical data, using

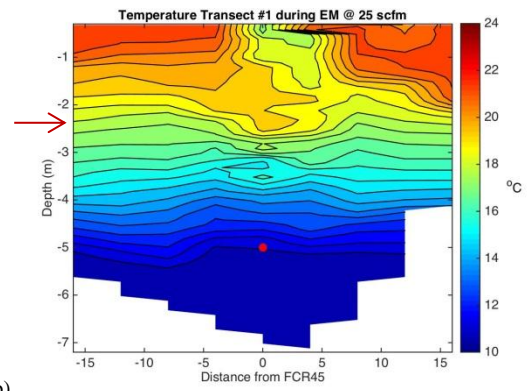
the profiles at site FCR50 (Figure 1) based on the assumption of horizontal homogeneity across the reservoir for water temperature. The results show that mixing induced by the EM system reduced the thermal stability to a large extent even though the diurnal variation of the air temperature above the water surface remained more or less similar over the study period (see Figure 5a). The result from the numerical data generally shows a consistent trend with the experiment.

Figure 6 shows the temperature profiles across Transect #1 that consists of nine single water column profiles evenly distributed over the 32-m wide cross-section over the EM diffuser (see Figure 1). Compared with the time series of the temperature profiles shown in Figure 4, a similar trend of the thermocline development can be observed at the two selected time instants before and during the EM mixing. It is clear in Figure 6b that the temperature profiles above the EM diffuser were affected by the bubble plumes, manifesting as a cluster of packed isotherms between the depth of the diffuser line and the DMPR (indicated approximately by the red arrow). It is believed that the pattern is caused by the entrainment and detrainment processes of the plumes, which enhance heat transfer across vertical layers of the water body.

In summary, the mixing by the SSS system does not disturb the temperature structure while adding oxygen to the hypolimnetic water, whereas the EM system deepens the thermocline and reduces the thermal stability across the reservoir. The coupled Si3D hydrodynamic model predicts well the experimentally observed scenarios.



a)



b)

Figure 6 Field temperature profiles at Transect #1: a) Before EM operation; b) 0.5 h during EM operation. The red arrow indicates the estimated DMPR from the field experiment.

Substance Transport

To analyse the substance transport induced by the mixing, the water quality variable turbidity is examined. Turbidity is a measure of the quantity of particles suspended in water that scatter light, decreasing water transparency. In FCR, high

turbidity may be an indicator of high nutrient concentrations, including particulate organic nitrogen and particulate organic phosphorus. The nutrient content in reservoirs may lead to eutrophication, which is the potential cause of algal blooms and hypoxia.

It has been observed above that significant mixing is caused by EM mixing during the experimental period. Therefore, the EM system is the focus of this investigation as the SSS system only mixes the hypolimnetic water.

The mass balance for the turbidity is achieved using the turbidity data collected from the CTD in the *in-situ* experiment. The calculation uses all the data from Transects #1-4 consisting of the profiles from 36 individual water columns across the entire reservoir. The total turbidity is estimated as follows:

$$m = \iint_{z_{sed}}^{z_{surf}} \bar{s} \cdot dh \cdot dA$$

where m is the total turbidity; \bar{s} represents the layer-average turbidity level; h is the water depth; A is the area of the water layer in the reservoir; and z_{surf} and z_{sed} are elevations from water surface to sediment. To calculate the average turbidity over the entire reservoir, we use:

$$\bar{C} = m/V$$

where \bar{C} is the average turbidity in NTU (Nephelometric Turbidity Units); and V is the volume of the reservoir. The average turbidity is calculated and plotted in Figure 7 for three representative time points before, during, and after the experiment.

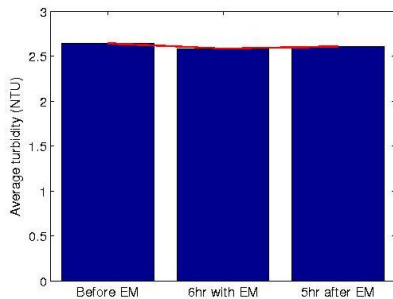


Figure 7 Turbidity mass balance during the EM mixing period.

Figure 7 suggests that the overall turbidity level over the EM experimental period was generally conserved, which means that the variation of turbidity distribution across FCR may be used to indicate substance transport even though the mechanisms driving water clarity (e.g. particulate matters and plankton) may have varied over time. Therefore, further investigation of the substance transport over the reservoir is carried out based on the field turbidity data in conjunction with the numerical tracer analysis using the Si3D hydrodynamic model.

Figure 8 shows the field turbidity and numerical tracer across FCR10-50 in two selected time points before and during the EM system in operation. It is observed that the substance which is initially near the littoral region of FCR is carried away by the flows induced by artificial mixing. The observation shows that the substance in the water layer between -3 and -2 m depth was displaced by the flows induced by the EM mixing. As a consequence, the substance was transported from the littoral region of FCR to the deep region around the depth of the EM diffuser (Figure 8c). It is believed that a counter-clockwise flow circulation in the metalimnion is formed by the detrained water towards the littoral region from the EM diffuser. The result shows that the induced circulation by the EM mixing enhances substance exchange between the shallow and deep regions.

The three-dimensional numerical results of tracers show a consistent trend with the field turbidity data. In the numerical model, tracers are injected into the water body at the location of the highest field turbidity one day before the EM system is turned on. The simulated pattern of the tracers in Figure 8d indicates the flow circulation similar to that observed in the experimental results (Figure 8c). This further confirms the enhancement of substance transport between the littoral and deep regions by the EM mixing.

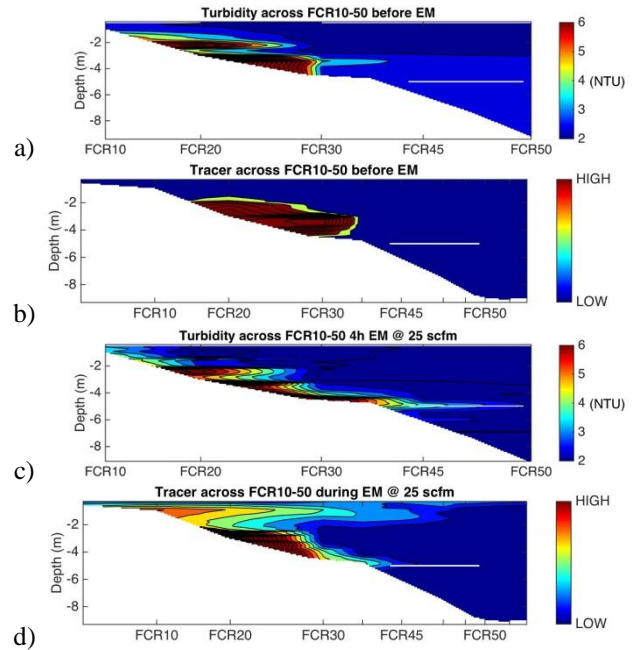


Figure 8 Field turbidity (a, c) and numerical tracer (b, d) in the longitudinal section across the reservoir from FCR10-50.

Conclusion

The preliminary investigation in this study has demonstrated that the mixing by the SSS does not substantially affect the thermal structure during the study period, whereas the EM mixing over a short duration deepens the thermocline and reduces the thermal stability significantly. The numerical results obtained from Si3D show a consistent trend with the experimental findings in terms of temperature structure. The field data shows that turbidity is a good tracer for visualising artificial mixing in the short term. It is found from both the experimental and numerical results that the EM mixing enhances the substance transport across the reservoir. This study has provided useful information for reservoir management of FCR.

References

- [1] Gerling, A. B., et al. First report of the successful operation of a side stream supersaturation hypolimnetic oxygenation system in a eutrophic, shallow reservoir, *Water Research*, **67**, 2014, 129-143.
- [2] Idso, S. B. On the concept of lake stability, *Limnology and oceanography*, **18**, 1973, 681-683.
- [3] Morton, B. R., Taylor, G. and Turner, J. S. Turbulent Gravitational Convection from Maintained and Instantaneous Sources, *Proceedings of the Royal Society of London. Series A. Mathematical and Physical Sciences*, **234**, 1956, 1-23.
- [4] Nürnberg, G. K., LaZerte, B. D. and Olding, D. D. An Artificially Induced Planktothrix rubescens Surface Bloom in a Small Kettle Lake in Southern Ontario Compared to Blooms World-wide, *Lake and Reservoir Management*, **19**, 2003, 307-322.
- [5] Rueda, F. J., Sanmiguel-Rojas, E. and Hodges, B. R. Baroclinic stability for a family of two-level, semi-implicit numerical methods for the 3D shallow water equations, *International Journal for Numerical Methods in Fluids*, **54**, 2007, 237-268.
- [6] Singleton, V. L., Gantzer, P. and Little, J. C. Linear bubble plume model for hypolimnetic oxygenation: Full-scale validation and sensitivity analysis, *Water Resources Research*, **43**, 2007.
- [7] Toffolon, M. and Serafini, M. Effects of artificial hypolimnetic oxygenation in a shallow lake. Part 2: Numerical modelling, *Journal of Environmental Management*, **114**, 2013, 530-539.